J Nanopart Res (2020) 22: 46
https://doi.org/10.1007/s11051-020-4750-8

RESEARCH PAPER

Three-dimensional printer emissions and employee exposures to ultrafine particles during the printing of thermoplastic filaments containing carbon nanotubes or carbon nanofibers

Kevin L. Dunn · Kevin H. Dunn · Duane Hammond · Samuel Lo

Received: 15 May 2019 / Accepted: 2 January 2020 / Published online: 7 February 2020

Abstract Recent studies have reported emission rates of up to 10^{12} ultrafine particles/min from fused filament fabrication three-dimensional printers when operated in unventilated or minimally ventilated test chambers. However, in these studies, there are no data to relate this rate to airborne concentrations in a manufacturing environment. An assessment of particle exposures of workers was conducted at a three-dimensional printing shop using multiple fused filament printers with unfilled and carbon nanotube and/or carbon nanofiber-infused polyetheletherketone filaments. The study simultaneously evaluated emissions in two environments: (1) in a field portable test chamber with one three-dimensional printer and (2) in the manufacturing area with multiple printers in use. Emission rates were calculated for a variety of filaments and ranged from 1.21 to 33.5×10^{11} particles/min, with geometric mean diameters ranging from 11.4 to 33.3 nm. The emission rates estimated by a scanning mobility particle sizer were much lower than from the fast mobility particle sizer due to differences in the lower size resolution. Samples collected in the chamber and manufacturing area by thermophoretic sampling included free (no polymer) carbon nanotubes and nanofibers and their bundles. The company reportedly never handled free carbon nanotubes or nanofibers, and prior research has indicated that the release of free nanomaterials through three-dimensional printing or mechanical action is highly unlikely. This presents the possibility that these materials are being released from the matrix during use or that these materials were brought into the facility through the supply chain, or by other means.

Keywords 3D printing · Air sampling · Carbon nanotubes · Engineering controls · Exposure assessment

Introduction

Multiple studies have shown that desktop three-dimensional (3D) printers emit nanoparticles and other compounds such as volatile organic compounds (VOCs), polycyclic aromatic hydrocarbons (PAHs), and metal dusts into the work environment (Afshar-Mohajer et al. 2015; Azimi et al. 2016; Kim et al. 2015; Mendes et al. 2017; Stephens et al. 2013; Yi et al. 2016; Zhang et al. 2017; Zhou et al. 2015). However, these studies are limited in scope and have not related the findings to a manufacturing environment, where multiple printers and filament combinations may be in use at the same time. Moreover, none of the previous studies have evaluated controlled chamber emissions and particle counts during normal operating conditions in the same manufacturing environment simultaneously while 3D printing, using carbon nanofiber (CNF) and carbon nanotube (CNT) infused filaments.

K. L. Dunn · K. H. Dunn (✉) · D. Hammond · S. Lo
National Institute for Occupational Safety and Health, 1090 Tusculum Avenue, Cincinnati, OH 45226, USA
e-mail: kdunn@cdc.gov

In 2013, Stephens et al. published the first known measurements of emissions of ultrafine particles (UFPs: particles smaller than 100 nm in diameter) resulting from the operation of a single make and model of commercially available desktop 3D printer (Stephens et al. 2013). In 2015 and 2016, five additional studies were published documenting nanoparticle and ultrafine particle emissions up to 10^{12} particles/min from multiple models of desktop 3D printers (Afshar-Mohajer et al. 2015; Azimi et al. 2016; Kim et al. 2015; Steinle 2016; Zhou et al. 2015). One of the studies found a single 3D print also resulted in emissions of VOCs such as styrene and methyl methacrylate, PAHs such as fluoranthene and pyrene, and 100–300 nm diameter particle emissions containing iron (Fe) and zinc (Zn) (Steinle 2016). An investigation into the aerosol dynamics and formation mechanisms for ultrafine particles emitted from 3D printers indicate that they may come from the condensation of vapors from the heated filaments onto preexisting particles or from filament additives (Zhang et al. 2018). Likewise, Gu et al. showed that large numbers of ultrafine particles are emitted from particles during 3D printing and that these particles are primarily composed of semi-volatile compounds derived from filament additives (Gu et al. 2019). As new 3D printing technologies are developed, novel materials with unknown toxicological properties will require appropriate risk management approaches, as occupational health risks associated with additive manufacturing are not yet clearly understood.

Initial 3D printing studies report measurements of nanoparticles and other emissions that indicate that there is reason for caution. To respond to this data gap, the National Institute for Occupational Safety and Health, (NIOSH) Nanotechnology Research Centers Advanced Materials and Manufacturing field team performed this exposure assessment study during the course of normal employee work activities associated with 3D printing in the manufacturing area, while simultaneously evaluating the particle emission rate from a single 3D printer also located in this area. This study's goal was to characterize emissions of ultrafine particles, carbon nanotubes (CNTs), and carbon nanofibers (CNFs) from one printer in an isolated chamber that was exhausted into the manufacturing environment. The second objective of this study was to assess workplace air concentrations of these particles in that manufacturing environment with multiple 3D printers operating simultaneously.

Methods

Facility/process description

The approximately 465-m^2 (5000 ft^2) plant had about 20 employees and produced 3D printed products using thermoplastic filaments containing CNTs or CNF. The facility included a development and manufacturing area (used for production-volume 3D printing), a robot research room, and a laser 3D printing research room. The facility also had several office and conference room spaces separate from the manufacturing areas. At the time of this evaluation, the manufacturing area had six fused filament fabrication (FFF) 3D printing machines. Each 3D printer was similar in design and included a heated build plate, a heated nozzle, an extruder, and an enclosure with an open top to allow filament to enter from an external filament spool. The build volume of each printer in the manufacturing area was 28 cm (width) × 27 cm (length) × 23 cm (height). The 3D printing process involved melting thermoplastic filament at high temperature, then injecting the filament through 0.5- or 0.25-mm diameter nozzles onto a heated build plate. The thermoplastic filaments used in the machines were 1.75-mm in diameter and supplied in 1 or 2 kg spools provided by an off-site vendor.

The primary manufacturing activities conducted involved 3D printer setup, 3D printing, post-build processing, and housekeeping. Printer set up included loading filament into the extruder, adjusting build equipment inside the machine, and setting up the computer. Post-build activities included removing parts from the build plate, cleaning the build plate, and cleaning filament extruder nozzles. These activities occurred in the manufacturing area, during normal working hours and are included in the area sampling data.

The manufacturing area was approximately 82 m^2 (885 ft^2) with a ceiling height of 3.7 m (12 ft). In addition to a general ventilation system, a canopy hood was located against one wall approximately seven feet above two of the six 3D printers (Fig. 1). The canopy hood exhausted air directly to the outdoors at a location at least 7.6 m (25 ft) away from outdoor air intakes. The canopy hood had a 61-cm-by-183-cm (24 in by 72 in) opening and was connected to two 46-cm (18 in) diameter ducts that exhausted to the outdoors. Air velocities were measured at the face of the canopy hood in ten equal areas using a multi-function ventilation meter (Model 9555, TSI, Inc., Shoreview, MN) outfitted with a hot wire transducer. These velocities were then averaged, resulting in an average face velocity of 1.5 m/s (304 ft./min) and a calculated volumetric flow rate of 103 m^3/min (3650 ft^3/min).

Five supply air diffusers and three return air grills were located in the ceiling of the manufacturing room. Airflow from each diffuser or grill was measured using an airflow capture hood (Model EBT731, TSI, Inc., Shoreview, MN). Results from air flow measurements showed that 31 m^3/min (1100 ft^3/min) of air was being supplied to the manufacturing area through the supply air diffusers in the ceiling, and 42 m^3/min (1500 ft^3/min) of air was being exhausted through the return air grills located along the wall and ceiling of the manufacturing area. Combined results from the canopy hood and return air grills showed that approximately 146 m^3/min (5150 ft^3/min) of air was being exhausted from the manufacturing area with only 31 m^3/min (1100 ft^3/min) of air being supplied. It should be noted that the ventilation system for this facility was controlled by the leasing agent, and researchers were not able to gather specific information such as percentage of outdoor air used in makeup air. An average of 29 air changes per hour (ACH) was calculated for the manufacturing area on the basis of the room volume and exhaust airflow rate.

Workplace characterization

The workplace characterization included observation of all tasks conducted during the FFF 3D printing, including reprocessing and cleaning extruder nozzles, and cutting or post-processing 3D printed parts. Up to six FFF 3D printers were operating at any time, with longer print times and printing products that were larger than the test bars printed in the chamber studies. In addition, a chamber test was conducted to help characterize the emissions from a single 3D printer located in the primary manufacturing area. Particle emission rates were calculated for the chamber environment, and particle size distributions were measured for both the chamber and manufacturing environments, using real-time particle instrumentation.

Direct reading and filter-based air sampling (described below) data was collected in the production area for the entire work shift of approximately 9 h with two to five printers in operation (not including the chamber). Additionally, air sampling was also conducted in a conference room separated from the production area for the entire shift to provide background information. Air sampling with the direct reading instruments was continuously conducted in the chamber for each shift, but with each distinct build analyzed independently. Filter-based air sampling was conducted separately for each build in the chamber and lasted from 16 min to 2.5 h depending on the build process—shorter times were from print failures and longer times when the full print was completed.

Filter-based particle air sampling

Full-shift personal and area air samples were collected for measurement and identification of airborne particles. While up to five operators may work in the manufacturing area at any given time, only two operators stayed in the manufacturing area for the majority of the work shift. During the first day of sampling, one of these primary operators volunteered to wear personal samplers and on day 2, both of these operators were sampled. Area air samples were also collected on both days, in fixed locations in the manufacturing shown in Fig. 1. In addition, office areas were also sampled to determine whether process emissions were migrating out of the manufacturing area.

Sampling for polymer aerosols and CNTs/CNFs was performed using preloaded cassettes (BestCheck, part number 225-321A, SKC Inc., Eighty Four, PA) consisting of 25-mm diameter, 0.8 μm pore size mixed cellulose ester (MCE) membrane filters mounted in open-face polypropylene conductive cassettes, with pumps operated at a flow rate of 3.0 L/min. The MCE samples were changed at 4-h intervals at the request of the microscopists to provide optimal loading for identification of particles. These samples were analyzed on a field emission electron microscope (Model 2100F, JEOL, Tokyo, Japan) in transmission electron microscope and scanning transmission electron microscope modes according to modified NMAM Method 7402 to identify the presence of polymer particulate, CNTs, and CNFs (NIOSH 2017). The analytical method modifications included eliminating the steps associated with the identification of asbestos. Three TEM grids were prepared from each MCE sample filter using a Jaffee wick washer technique. In general, to be acceptable for analysis, the grid should have at least 75% intact grid openings and a particle loading less than about 25% (area coverage). A total of 13 to 15 openings per grid were viewed to identify particle structures.

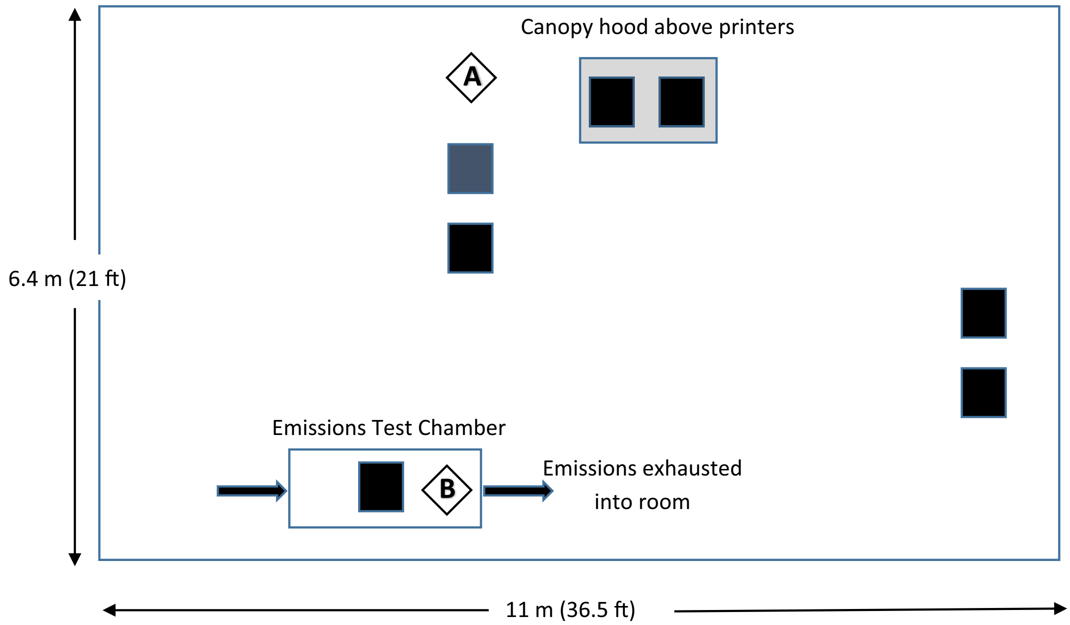

Fig. 1 Manufacturing area layout with printer and area sampling locations. Note: Printer locations are indicated by ■. Area samples Ⓐ included filter and thermophoretic samples (TPS) for microscopy and a Nanoscan SMPS for particle sizing. These samplers were approximately 1 m (3 ft) from the closest printer. Area samples Ⓑ (inside the chamber) included filter and thermophoretic samples (TPS) for microscopy, a Nanoscan SMPS, and a fast mobility particle sizer (FMPS) for particle sizing.

Since the particles of interest consisted of several distinct types, polymer alone, polymer with embedded CNT or CNF, or free CNT/CNF, it was not practical to estimate a count of particles, and results were given qualitatively as "present" or "not present" on the air sample. Because the filaments contained small quantities of CNTs physically bound in the thermoplastic, microscopic analysis was used rather than a mass-based elemental carbon method to identify the presence of CNTs. Large amounts of polymer relative to CNT tend to overwhelm the elemental carbon, making detection of CNT by elemental carbon analysis, in these circumstances, difficult or impossible.

Thermophoretic sampling

Thermophoretic samplers (TPS) developed by Colorado State University and the RJ Lee Group were also used to collect manufacturing area and chamber samples for microscopy (Leith et al. 2014). Airborne particles pass through a temperature gradient, where the particles move in the direction of decreasing temperature and deposit on the colder side of the flow channel, directly onto a TEM grid. The sampler is size-selective for particles below 300 nm and draws in air at 0.005 L/min (Leith et al. 2014). The TPS samples were analyzed by TEM to identify CNT structures. In total, 16 MCE samples (seven area, five personal, and four chamber) and 12 TPS samples (eight chamber, two chamber exhaust, and three area) were collected for TEM analysis.

Emission characterization and rate estimation-chamber test

Particle emissions were measured from a single 3D printer in a 0.34-m^3 (12 ft^3) test chamber (Fig. 2) assembled on-site to enclose a representative 3D printer with a build volume of 25 cm (width) × 16 cm (length) × 15 cm (height). The materials evaluated in the 3D printing process consisted of proprietary thermoplastic filaments that contained either 25% CNTs (CNT25), 30% CNF (1KHFC30), 10% CNF (1KHFZ), proprietary filament (1AR2), or unfilled polyetheretherketone (PEEK). Air entering the chamber passed through a portable floor fan (Model SS-400-PYT, Sentry Air Systems Inc., Cypress, TX) with a high-efficiency particulate air (HEPA) filter (Model SS-400-HF, Sentry Air Systems Inc., Cypress, TX) and then exhausted back into the manufacturing area without additional filtration (Fig. 2). A fast mobility particle sizer (FMPS) and a

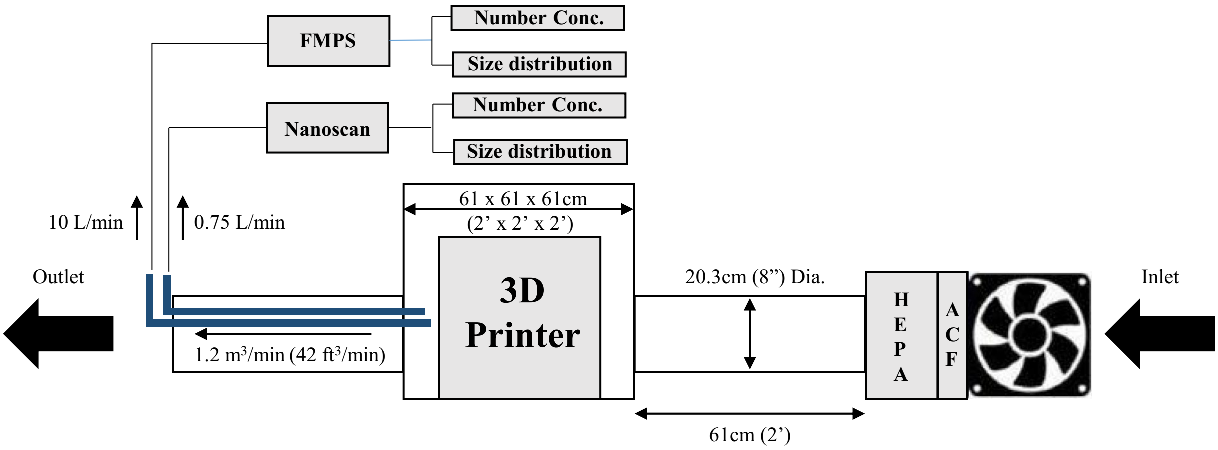

Fig. 2 Portable isolation chamber used for evaluating printer emissions from a series of different filaments

scanning mobility particle sizer (SMPS) were used to measure and characterize emissions in the exhaust duct outlet of the chamber.

The TSI NanoScan SMPS (Model 3910, TSI Inc., Shoreview, MN) directly measured ultrafine particle numbers and sizes (ranging from 10 to 420 nm in diameter) in 13 size channels using electrical mobility with a 0.75-L/min sample flow rate. The lower and upper particle concentration measurement limits range from 100 to 1,000,000 particles/cm^3. A TSI FMPS (Model 3091, TSI Inc., Shoreview, MN) measures particles from 5.6 to 560 nm in 32 size channels with a flow rate of 10 L/min. This instrument provides a fast response rate (1 s) and a high sampling flow rate (10 L/min) minimizing diffusion losses of ultrafine particles to the tubing surface. It uses an electrical mobility measurement technique similar to that used in NanoScan, but the FMPS spectrometer uses multiple, low-noise electrometers for particle detection instead of a condensation particle counter. During the printer emission characterization, the NanoScan logged the total number concentration and size distribution each minute, while the FMPS recorded this information every second.

Emission rate calculations

Emission rates were calculated from the 3D printer in the portable chamber using the method published by Mendes et al. (Mendes et al. 2017). The method assumes that the high airflow rate through the chamber results in turbulent well-mixed air and that measured particle concentrations correspond to fresh emissions. When the airflow rate through the chamber is known, the particle emission rate, E, can be calculated using Eq. 1:

$$E = NQ \quad (1)$$

where N is the particle number concentration and Q is the air flow rate at the outlet of the chamber. The particle concentrations were adjusted for diffusion losses in the sampling lines using the methods outlined by Kulkarni et al. (2011). Diffusion losses in the 0.5 m (1.6 ft) long sampling tubes were less than 9% for the Nanoscan and less than 4% for the FMPS at the smallest size bins (corresponding to the highest loss of any particle size by percentage). Geometric mean particle size and geometric standard deviations were computed using the Nanoscan and FMPS software programs (Nanoscan manager software version 1.0.0.19 and FMPS software version 3.1.0.0).

Results

Workplace characterization

Filter-based and TPS air sampling

Personal and area air sampling results collected on MCE filters for the microscopy analysis is shown in Table 1. Polymer particles containing CNF/CNT were found in all samples (Fig. 3), but free CNTs were only found on one office area sample and on one personal sample (Fig. 4) from a 3D printer operator. However, the office area sample had been inadvertently attached to the 3D

Table 1 Results of personal and area air sampling for particles with MCE filters

Sampling location and time	3D printing material	CNT no polymer	CNF no polymer	Polymer with CNT/CNF	CNT&CNF Bundles no polymer
Day 1 personal samples					
Operator 2, AM	1KHFZ/1AR2/1KHFC30/CNT25			x	
Operator 2, PM	1KHFZ/1AR2/1KHFC30/CNT25			x	
Day 1 area samples					
Manufacturing area, AM	1KHFZ/1AR2/1KHFC30/CNT25			x	
Office, AM[a]	–	x		x	
Manufacturing area, PM	1KHFZ/1AR2/1KHFC30/CNT25			x	
Office, PM				x	
Day 2 personal samples					
Operator 1, AM + PM	1KHFZ/1KHFC30/CNT25/PEEK			x	
Operator 2, AM	1KHFZ/1KHFC30/CNT25/PEEK			x	
Operator 2, PM[b]	1KHFZ/1KHFC30/CNT25/PEEK	x		x	
Day 2 area samples					
Office	–			x	
Manufacturing area	1KHFZ/1KHFC30/CNT25/PEEK			x	
Manufacturing area	1KHFZ/1KHFC30/CNT25/PEEK			x	
Chamber sampling					
Inside chamber	1KHFC30			x	
Inside chamber	1KHFC30			x	
Inside chamber	1KHFC30			x	
Inside chamber	CNT25			x	

Empty cell indicates that material was not found on the specified sample

[a] Area air sample collected from the office was accidently attached to operator 2 for about 2 min. This could have resulted in cross-contamination from the manufacturing area

[b] This sample also contained silica

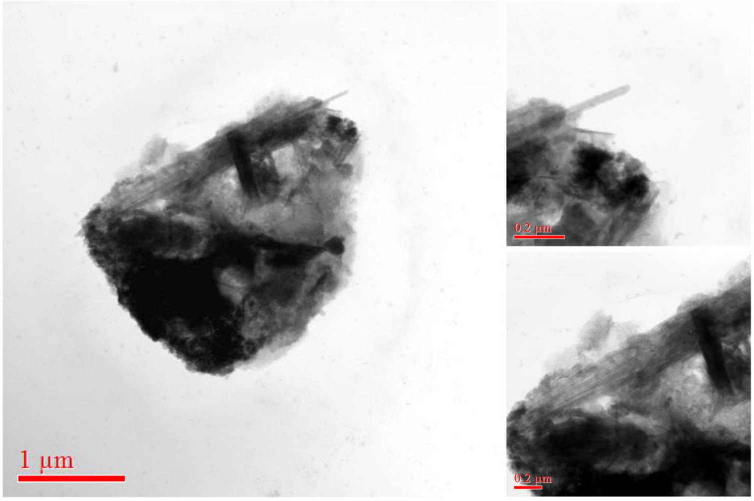

Fig. 3 STEM image of a polymer fragment containing embedded CNT/CNF structure in the office area MCE sample. Right side images are close ups of left side image

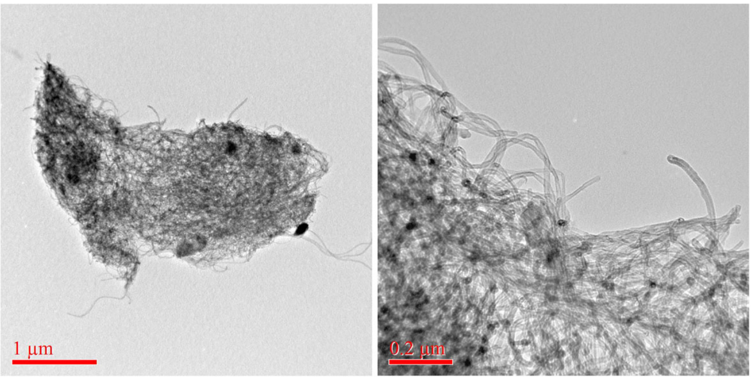

Fig. 4 Microscopy results showing approximately 20 nm diameter CNT structure collected on a personal MCE sample. Right side image is close up of left side image

printer operator for about 2 min during a media change out, so the CNT may have come from the manufacturing area. Operators do enter both areas throughout the day, so it is not possible to attribute the free CNT to only one area based on these results. Results from manufacturing area air samples collected with the TPS samplers are shown in Table 2. On day 1, only polymer fragments were found in the manufacturing area sample collected in the morning, but clean CNT and CFs were found in the area sample collected in the afternoon. On day 2, free CNT/CNFs and bundles of those materials were found in the manufacturing area. The personal sample on Operator 2 showed free CNT on day 2, as well.

The chamber results showed differences between the MCE filter and TPS sample results. For example, polymer-free CNT, CNF, or both CNT/CNF structures were identified in all but one TPS air sample, but free CNT or CNF structures were not found in the co-located MCE samples collected in the chamber. Figure 5 shows CNT/CNF clusters found in TPS samples, and Fig. 6 shows images of CNT/CNF bundles also found in TPS samples. This indicates that polymer-free CNTs or CNT/CNF agglomerates may be emitted during printing with these filament materials and may not be detected using MCE filter-based methods.

Table 2 Results from area samples collected with the TPS samplers

Location	Material	CNT only no polymer	CNF only no polymer	Polymer with CNT/CNF	CNT&CNF Bundles no polymer
Day one area samples					
Manufacturing area	1KHFZ/1AR2/1KHFC30/CNT25	x	x	x	
Chamber studies					
Chamber run	1AR2	x			
Chamber run	1KFCH30				
Chamber run	1KFCH30	x			x
Day two area samples					
Manufacturing area	1KHFZ/1KHFC30/CNT25/PEEK	x			x
Chamber studies					
Chamber run	1KFCH30	x		x	x
Chamber run	1KFCH30	x			x
Chamber run	1KHFC30			x	
Chamber run	1KFCH30	x			
Exhaust	CNT25	x			x
Chamber run	CNT25			x	

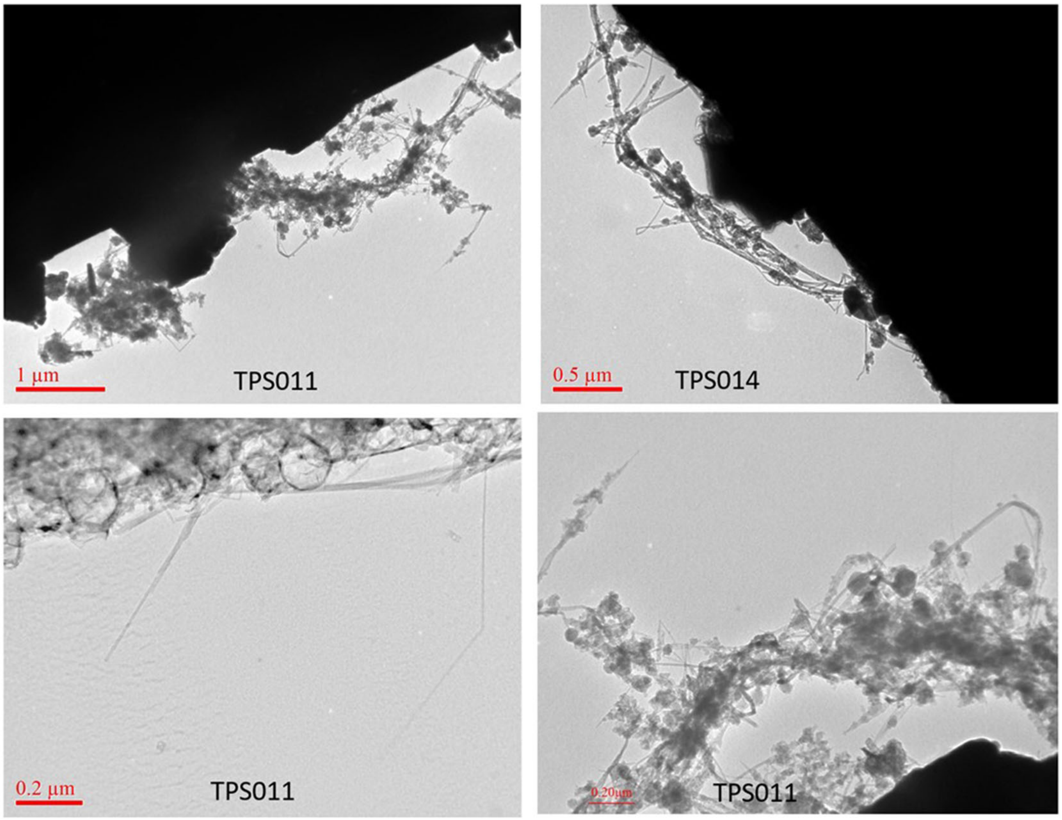

Fig. 5 TEM images of CNT/CNF clusters found in TPS samples for the 5th chamber run (1KHFC30, TPS011) and for the 2nd chamber run (CNT25, TPS 014)

Emission characterization and rate estimation-chamber test

Emission rate calculations by material and instrument type (NanoScan or FMPS) are shown in Table 3, along with the geometric mean diameter and geometric standard deviation of ultrafine particles from the particle size distribution data. Figure 7 shows the time series of particle emissions measured by the NanoScan SMPS during 2 days of sampling, with the darker line showing continuous printing operations in the manufacturing area and the lighter line showing continuous air sampling in the chamber. Despite the large peaks of particle concentrations seen in the chamber, the corresponding concentrations measured in the manufacturing area did not show significant elevations except when an

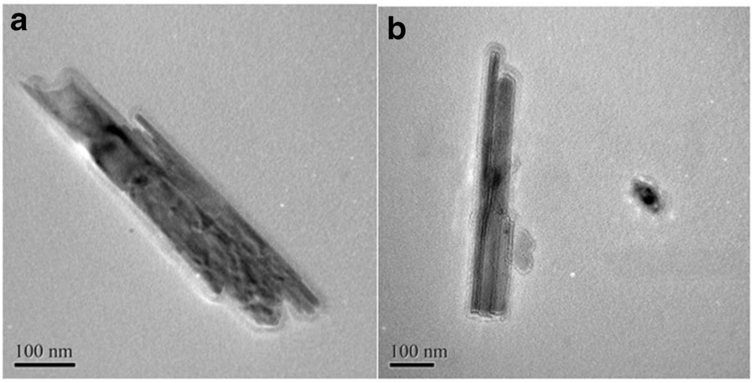

Fig. 6 TEM images of CNT/CNF bundles found in TPS samples in **a** the manufacturing area in day 2 (left image) and **b** the chamber exhaust in day 2 (right image)

Table 3 Geometric mean diameter, geometric standard deviation, and nanoparticle emission rates from 3D printing with CNT, CNF, and unfilled materials

Chamber Run no.	Shift	Filament	Instrument	FMPS % of particles < 10 nm	Geometric mean diameter (nm)	Geometric standard deviation	Emission, particles/min
	Night 1	Manufacturing area[a]	NanoScan		36.3	1.72	[b]
		Office area[a]	NanoScan		54.2	1.61	[b]
1	Day 1	Without 3D printing	NanoScan		50.9	1.45	
2		1AR2	NanoScan		33.3	1.38	2.25×10^{11}
2		1AR2	FMPS		[c]	[c]	[c]
3		1KHFC30	NanoScan		22.5	1.34	4.15×10^{11}
3		1KHFC30	FMPS	30%	14.2	1.50	9.42×10^{11}
4		CNT25	NanoScan		22.4	1.37	1.81×10^{11}
4		CNT25	FMPS	50%	11.9	1.44	6.36×10^{11}
5		CNT25	NanoScan		22.8	1.38	1.61×10^{11}
5		CNT25	FMPS	39%	12.7	1.48	5.65×10^{11}
6		CNT25fail 1	NanoScan		26.2	1.44	9.84×10^{11}
6		CNT25fail 1	FMPS	16%	21.1	1.71	2.14×10^{12}
7	Day 2	PEEK	NanoScan		27.4	1.51	8.16×10^{11}
7		PEEK	FMPS	26%	13.9	1.58	1.51×10^{12}
8		PEEK	NanoScan		27.5	1.49	9.12×10^{11}
8		PEEK	FMPS	27%	14.6	1.57	2.02×10^{12}
9		1KHFZ	NanoScan		28.9	1.52	6.72×10^{11}
9		1KHFZ	FMPS	46%	12.7	1.51	1.62×10^{12}
10		1KHFC30	NanoScan		28.5	1.53	1.57×10^{12}
10		1KHFC30	FMPS	14%	18.5	1.64	3.35×10^{12}
11		CNT25 fail 2	NanoScan		29.1	1.49	7.02×10^{11}
11		CNT25 fail 2	FMPS	11%	20.8	1.77	1.96×10^{12}
12		CNT25 fail 3	NanoScan		22.7	1.45	4.01×10^{11}
12		CNT25 fail 3	FMPS	47%	12.1	1.45	1.11×10^{12}
13		CNT25	NanoScan		23.7	1.38	1.21×10^{11}
13		CNT25	FMPS	58%	11.4	1.42	4.20×10^{11}

[a] Measurements made outside of the chamber; all other measurements in the table are from inside the chamber

[b] Emission rates were not calculated for measurements taken outside of the chamber. Conclusions were based on direct reading data

[c] The FMPS arrived to the field study site late and was not available for the 1AR2 chamber run

employee cut tensile bars with a rotary tool. This indicates that the printer emissions from the chamber were damped out by both the room volume and general ventilation system.

The chamber tests represented in Fig. 7 began at 10:25 a.m. by heating the build plate and operating the 3D printer without any filament in the extruder. This test was conducted to determine if particles would be generated from moving belts or motors or by heating the nozzle and build plate. This test ended at 11:05 a.m. Concentrations in the chamber remained below approximately 80 particles/cm^3, indicating that these activities did not generate any measurable particle concentrations. After this background characterization run, 12 chamber runs were conducted during 2 days using five different filaments to 3D print tensile bars—note run numbers are listed in Table 3. Peak particle concentrations from 3D printing during the chamber tests ranged from less than 200,000 particles/cm^3 during runs 3, 4, and 5 to over 700,000 particles/cm^3 during runs 6 and 10 as shown in Fig. 7. During runs 3–5, 10, and 13 (using filaments filled with CNFs or CNTs), the total particle concentrations (as measured by the Nanoscan) were less than 350,000 particles/cm^3. During runs 2 and 7–9 (using

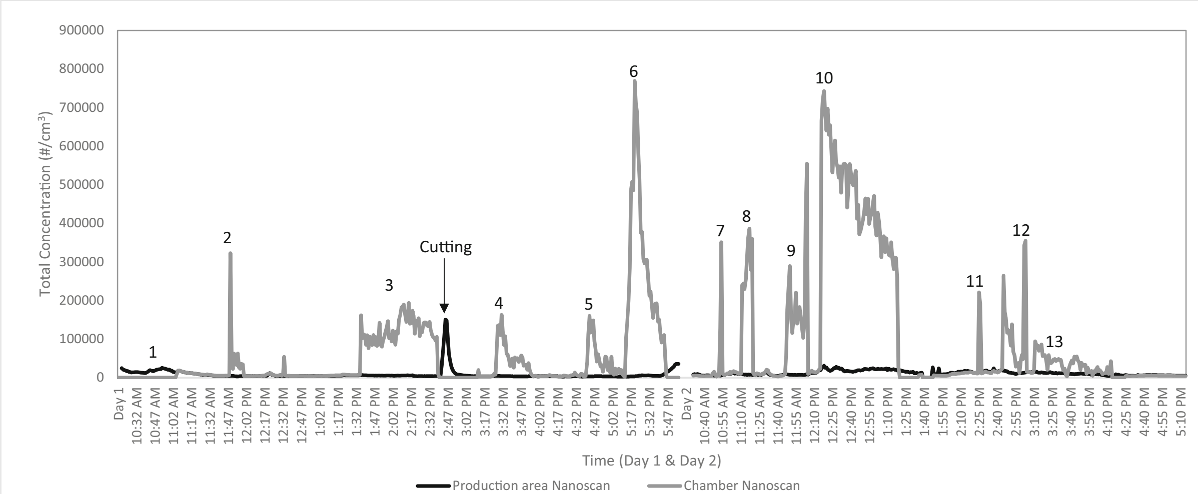

Fig. 7 Particle number concentration in the chamber and manufacturing areas during chamber testing using the Nanoscan. The numbers above the concentration plots correspond to different filament tests as shown in Table 3

unfilled thermoplastic filaments), the peak concentrations were generally around 400,000 particles/cm^3. The highest chamber concentrations were during run 6 which was a failed print using 25% CNT filament which peaked at over 700,000 particles/cm^3.

Figure 8 shows that the particle concentrations measured in the chamber by both the FMPS and Nanoscan. Figure 9 shows the particle size distribution from the Nanoscan in the chamber during runs using CNT filaments and the particle size distribution from the Nanoscan in the general production area. Although the upper size range of the Nanoscan and FMPS are both approximately 500 nm, the data indicate that the most particles were in the ultrafine range below 100 nm. The total concentration of particles measured in the chamber study using the FMPS was approximately twice as high as the concentrations measured using the NanoScan (Fig. 8; Table 3). One explanation is left censoring of particle sizes for the NanoScan; the FMPS can detect smaller particles (down to 5.6 nm) compared to the NanoScan (particle detection size limit of 10 nm). Therefore, the smaller particles to the left side of the size distribution curve could be counted by the FMPS but not by the NanoScan. This could help explain the difference between the concentrations measured by the two instruments. Between 11 and 58% of the particles measured by the FMPS were smaller than 10 nm as shown in Table 3, depending on filament material. In addition, the difference in the measurement range of these instruments affected the determination of GMD with the FMPS indicating GMDs about half the size of the Nanoscan.

Discussion

The chamber study showed that between 10^{11} and 10^{12} particles/min was emitted from one 3D printer during the printing of a standard tensile bar using a range of different filament materials. However, particle counts in the manufacturing area did not increase as a result of emissions from the chamber or when the six 3D printers were operating during the workplace evaluation. The results from the emission measurements and size distribution data in this study suggest that the room volume and the general ventilation of 29 ACH prevented the buildup of ultrafine particles from multiple 3D printers operating simultaneously in the manufacturing area. For comparison, laboratories typically have air change rates between 6 and 12 ACH depending on their design and operation (NRC 2011). Some researchers have found that increasing air change rates provides significantly reduced background contaminant levels (Klein et al. 2009; Schuyler 2009). However, general ventilation leaves opportunities for employees to be exposed to 3D printer emissions due to the distance between where particles are generated and where they are exhausted. Local exhaust ventilation at the source of emissions is

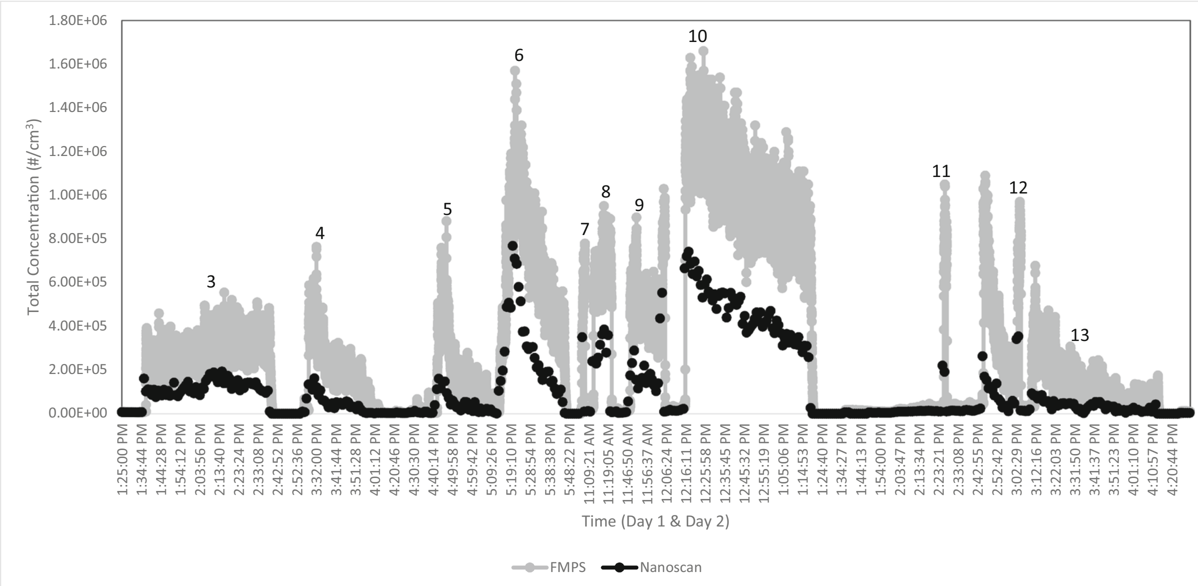

Fig. 8 Particle number concentration during chamber testing using the Nanoscan and FMPS. The numbers above the concentration plots correspond to different filament tests as shown in Table 3

more effective than general ventilation in controlling process emissions and reducing worker exposures.

While personal sample results were generally unremarkable, polymer particles containing CNT/CNFs were detected in the air in personal, office area, manufacturing area, and chamber samples indicating these particles are migrating throughout the facility. Moreover, free CNTs and CNFs (no polymer on the structures) were found on microscopy samples collected by TPS both in the chamber and manufacturing area, though the company had reportedly never handled free CNTs or CNFs in this facility. Although these results indicate that free CNTs and CNFs were released during 3D printing with the tested filaments, prior research suggests that the use of these materials during 3D printing is unlikely to release free CNFs/CNTs (Huang et al. 2012; Kang et al. 2017). This contradiction in findings supports the need for further examination. One explanation may be free CNT and

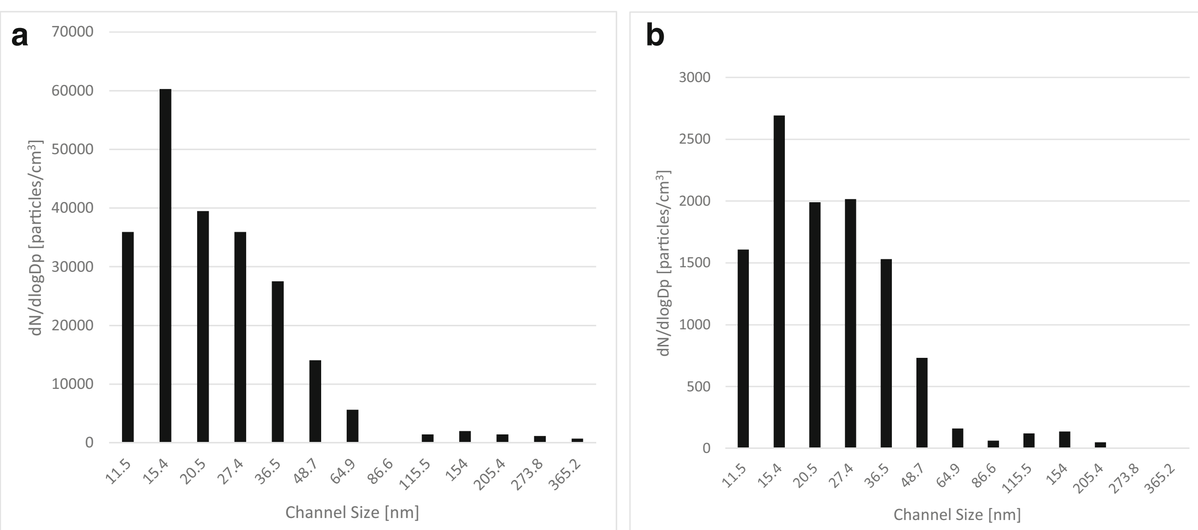

Fig. 9 Particle size distributions from the Nanoscan during sampling in the chamber (**a**) and production area (**b**)

CNF could be present on the filament surface or in the packaging materials from the manufacturer, or that new material compounds and uses could release nanomaterials in ways not previously seen. In addition, because the TPS samplers are designed to selectively sample particles smaller than 300 nm, they provide a more specific result than traditional filter-based methods when sampling for particle in this size range. However, this same design feature will not sample particles in the respirable size range, so using overlapping sampling techniques will provide the best representation of exposures.

Ultrafine particle concentrations exhibited high transient peaks during print failures, such as the one that occurred at 5:20 p.m. (run 6) on day 1 when 3D printing with CNT (Fig. 7). These results are similar to other research that also found increases in ultrafine particle concentrations during print failure while 3D printing with the base polymer without filler (Yi et al. 2016). This finding is important, because printer operators were observed leaning directly into the printer at these times trying to observe the process for detection or correction of an issue, presenting a potential exposure when the emissions rate was highest. Local exhaust ventilation and printer enclosures could potentially help reduce operator exposure to ultrafine particle concentrations during both 3D printing failures and normal operation. Figure 7 shows that particle counts decrease to below the limit of detection when the process is stopped either at failure or completion due to the high airflow rate through the chamber. This indicates that simple work practices, like waiting to approach the printer after stopping the process, could also reduce potential exposure situations.

Finally, particle count emission rates were between 1.8 and 3.5 times higher when measured with the FMPS compared to the NanoScan with between 11 and 58% of the particles emitted during the chamber tests below the measurement size range of the NanoScan (Table 3; Fig. 8). While this indicates that the FMPS measured emissions missed by the Nanoscan, this instrument is more suited to a laboratory environment and may not be an ideal instrument for use in field studies due to its size, weight, and power requirements. Most other published studies of 3D printing emissions only measured ultrafine particles with a resolution only down to the 10-nm size range. However, Mendes et al. also measured large numbers of particles smaller than 10 nm originating from 3D printing cycles (Mendes et al. 2017). Several other factors including channel resolution, flow rate, and measurement technique may result in variability between NanoScan and FMPS count data. The higher flow rate of the FMPS also minimizes diffusion losses of ultrafine particles to the sample tubing surface.

Conclusions

Ultrafine particles were generated during 3D printing regardless of the type of filaments used. Chamber measurements show emission rates in the hundreds of billions of particles/min, with up to 58% of the particles measured being smaller than 10 nm. The highest emission rates of ultrafine particles occurred at the start of the printing process and during failed prints. However, particle count concentrations in the chamber returned to background levels within 10 s from when the process stopped. Emission rates and size distribution measured with a NanoScan SMPS showed lower emission rates and GMDs when compared to the FMPS. This is due to a physical measurement limitation of the NanoScan which has a lower size resolution limit of 10 nm. Given the data from this study, it is important to understand the limitations of the real-time instruments used when assessing emission from 3D printers. The use of instruments with lower size detection limits of 10 nm (as do most SMPS instruments) can lead to a substantial underestimation of emission rates and overestimation of median particle sizes.

Concentrations of ultrafine particles in the manufacturing area did not increase above background even with all printers operating, likely because of general dilution and overall room volume. While we did not see an increase in ultrafine particle concentrations in the manufacturing area on the real-time instrumentation, ultrafine particles and nanomaterials were found in air samples analyzed by TEM. Free CNT and CNF without polymer were found in personal, area, and chamber samples collected by MCE filters and TPS, although these materials have never been used in the facility in a loose form. This presents the possibility that these materials are being released from the matrix during use, which has not been seen in previous studies, or that these materials were brought into the facility through the supply chain, or by other means.

Acknowledgments The authors would like to acknowledge the support and cooperation from the management and staff of the study sites. The authors are also grateful Drs. Bon Ki Ku and Aleks

Stefaniak for their insightful comments and suggestions on the early version of the manuscript, and Chen Wang for his contribution of the microscopic analysis and TEM images.

Disclaimer The findings and conclusions in this manuscript are those of the authors and do not necessarily represent the official position of the National Institute for Occupational Safety and Health, Centers for Disease Control and Prevention. Mention of any company or product does not constitute endorsement by the National Institute for Occupational Safety and Health, Centers for Disease Control and Prevention.

Funding information This research was funded by the National Institute for Occupational Safety and Health Nanotechnology Research Center.

Compliance with ethical standards

Conflict of interest The authors declare that they have not conflict of interest.

References

Afshar-Mohajer N, Wu C-Y, Ladun T, Rajon DA, Huang Y (2015) Characterization of particulate matters and total VOC emissions from a binder jetting 3D printer. Build Environ 93:293–301

Azimi P, Zhao D, Pouzet C, Crain NE, Stephens B (2016) Emissions of ultrafine particles and volatile organic compounds from commercially available desktop three-dimensional printers with multiple filaments. Environ Sci Technol 50:1260–1268

Gu J, Wensing M, Uhde E, Salthammer T (2019) Characterization of particulate and gaseous pollutants emitted during operation of a desktop 3D printer. Environ Int 123:476–485

Huang G, Park JH, Cena LG, Shelton BL, Peters TM (2012) Evaluation of airborne particle emissions from commercial products containing carbon nanotubes. J Nanopart Res 14: 1231

Kang J et al (2017) Generation and characterization of aerosols released from sanding composite nanomaterials containing carbon nanotubes. NanoImpact 5:41–50

Kim Y, Yoon C, Ham S, Park J, Kim S, Kwon O, Tsai P-J (2015) Emissions of nanoparticles and gaseous material from 3D printer operation. Environ Sci Technol 49:12044–12053

Klein RC, King C, Kosior A (2009) Laboratory air quality and room ventilation rates. J Chem Health Saf 16:36–42

Kulkarni P, Baron PA, Willeke K (eds) (2011) Aerosol measurement: principles, techniques, and applications, 3rd edn. Wiley, Hoboken

Leith D, Miller-Lionberg D, Casuccio G, Lersch T, Lentz H, Marchese A, Volckens J (2014) Development of a transfer function for a personal, thermophoretic nanoparticle sampler. Aerosol Sci Technol 48:81–89

Mendes L et al (2017) Characterization of emissions from a desktop 3D printer. J Ind Ecol 21:S94–S106

NIOSH (2017) NIOSH manual of analytical methods (NMAM). 5th ed. O'Connor PF, Ashley K (eds) Cincinnati: U.S. Department of Health and Human Services, Centers for Disease Control and Prevention, National Institute for Occupational Safety and Health, DHHS (NIOSH) Publication No. 2014-151

NRC (2011) Prudent practices in the laboratory: handling and management of chemical hazards. The National Academies Press, National Research Council, Updated Version Washington, DC

Schuyler G (2009) The effect of air change rate on recovery from a spill. Seminar

Steinle P (2016) Characterization of emissions from a desktop 3D printer and indoor air measurements in office settings. J Occup Environ Hyg 13:121–132

Stephens B, Azimi P, El Orch Z, Ramos T (2013) Ultrafine particle emissions from desktop 3D printers. Atmos Environ 79:334–339

Yi J, LeBouf R, Duling MG, Nurkiewicz T, Chen BT, Schwegler-Berry D, Virji MA, Stefaniak AB (2016) Emission of particulate matter from a desktop three-dimensional (3D) printer. J Toxic Environ Health A 79:453–465

Zhang Q, Wong JP, Davis AY, Black MS, Weber RJ (2017) Characterization of particle emissions from consumer fused deposition modeling 3D printers. Aerosol Sci Technol 51: 1275–1286

Zhang Q, Sharma G, Wong JPS, Davis AY, Black MS, Biswas P, Weber RJ (2018) Investigating particle emissions and aerosol dynamics from a consumer fused deposition modeling 3D prtinted with a lognormal moment aerosol model. Aerosol Sci Technol 52:1099–1111

Zhou Y, Kong X, Chen A, Cao S (2015) Investigation of ultrafine particle emissions of desktop 3D printers in the clean room. Proc Eng 121:506–512